Geomechanics and Engineering, *Vol. 24, No. 6 (2021) 559-572*
DOI: https://doi.org/10.12989/gae.2021.24.6.559

Measurements and analysis of load sharing between piles and raft in a pile foundation in clay

Kongpop Watcharasawe[1a], Pornkasem Jongpradist*[1], Pastsakorn Kitiyodom[2b] and Tatsunori Matsumoto[3c]

[1]*Construction Innovations and Future Infrastructures Research Center, Department of Civil Engineering, Faculty of Engineering, King Mongkut's University of Technology Thonburi, Thungkhru, Bangkok, Thailand*
[2]*Geotechnical & Foundation Engineering Co., Ltd. (GFE), Bangkok, Thailand*
[3]*Faculty of Geosciences and Civil Engineering, Kanazawa University, Kakuma-machi, Kanazawa, Japan*

(Received May 15, 2020, Revised February 8, 2021, Accepted March 18, 2021)

Abstract. This research presents the monitoring results and their interpretation on load sharing of the pile foundation during the construction of a high-rise (124 m in height) building in Bangkok, in soft clayey ground. Axial forces in several piles, pore water pressure and earth pressures beneath the raft in a tributary area were monitored through the construction period of the building. The raft of the pile foundation in soft clayey ground can share the load up to 10-20% even though the foundation was designed using the conventional approach in which the raft resistance is ignored. The benefit from the return of ground water table as the uplift pressure is recognized. A series of parametric study by 3D-FEA were carried out. The potential of utilizing the piled raft system for the high-rise building with underground basement in soft clayey ground was preliminarily confirmed.

Keywords: 3D FE; load sharing; monitoring; piled raft; soft soil

1. Introduction

Piled raft foundations have been widely utilized for several civil structures especially for buildings and bridges, as they have been demonstrated to be a cost-effective foundation system in conditions in which the soil underneath the raft can offer significant bearing capacity (e.g., Randolph 1994, Poulos 2001, Ko *et al.* 2018). Several buildings around the world have been successfully designed employing the concept of piled raft, particularly in Germany (Katzenbach *et al.* 2015) and Japan (Yamashita *et al.* 2011). Different design approaches including 1) conventional method, 2) creep piling method, 3) differential settlement control and 4) settlement reducing method have been introduced as reported by Randolph (1994), Russo (1998), Fioravante et al. (2008) and Russo (2018). Most of case histories were constructed on hard soil layers (sand or stiff clay layer) in which the raft can share the load up to 20 to 50% (e.g., Phung 2010).

In design of a pile foundation in soft soil area where the ground at shallow depth possesses low bearing capacity and the building settlement needs to be minimal, the pile foundations were mostly designed considering that the total load of structure is entirely carried by piles (e.g., Amornfa *et al.* 2012) based on the pile group concept. However, for high-rise buildings which usually require the basement floors for purposes of car parking and so on, pile foundation is constructed in a sufficiently firm layer at greater depths. In the construction, a raft is normally cast directly on the soil surface of excavated area so that a significant percentage of the load can be transmitted from the raft to the firm soil. A few applications of piled rafts in soft to medium ground have been reported (Tan *et al.* 2006, de Sanctis and Mandolini 2006, de Sanctis and Russo 2008, Yamashita *et al.* 2011, Khanmohammadi and Fakharian 2018). The case reported by de Sanctis and Russo (2008) shows that the raft placed on medium ground can support almost half of the total applied load. The case reported by Yamashita *et al.* (2011) shows that the raft placed on soft ground can share the load up to 40%. However, in this project the raft has been designed to work with the grid-form deep mixing walls. Moreover, the case studies cover only low-rise and medium-rise buildings.

Several numerical studies on load sharing behaviour indicated that the load shared by raft in soft ground can be in ranges from 10 to 20% (Amornfa *et al.* 2012, Watcharasawe *et al.* 2015, Khanmohammadi and Fakharian 2018). The design following the pile group concept ignoring the raft capacity becomes conservative and uneconomical. Not only the numerical analyses but also field monitoring of pile foundations (Kakurai *et al.* 1987, Yamashita and Kakurai 1991) have proved that the contribution of the raft can be significant. Up to date, there is no field monitoring of load sharing between the piles and raft of pile foundation of high-rise building in soft ground. Hence, it is difficult to confirm the potential of employing

∗Corresponding author, Associate Professor
E-mail: pornkasem.jon@kmutt.ac.th
[a]Ph.D. Candidate
E-mail: kongpop.wat@mail.kmutt.ac.th
[b]Ph.D.
E-mail: pastsakorn_k@gfe.co.th
[c]Professor
E-mail: matsumoto@se.kanazawa-u.ac.jp

ISSN: 2005-307X (Print), 2092-6219 (Online)

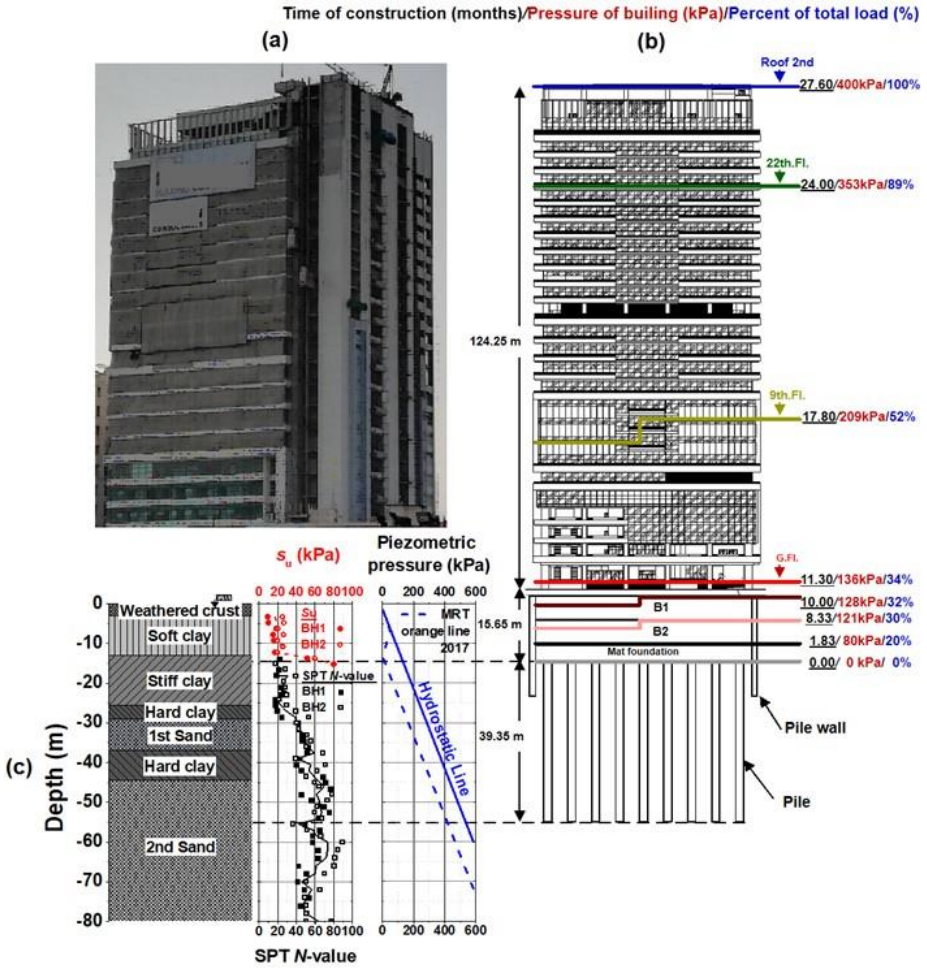

Fig. 1 Detail of building: (a) Building image, (b) Structural configuration of the building and construction time sequence and (c) Soil profile, standard penetration test (SPT) N values and piezometric pressure in Bangkok subsoil

the piled raft system in this ground condition. Moreover, under the load from the raft, the soil underneath the raft would undergo long term consolidation settlement for clayey soil. In some cities where the ground subsidence (such as from deep well pumping) is encountered, together with the consolidation settlement (Sales *et al*. 2010 and Fattah *et al.* 2013), the potential gap formation beneath the raft in long-term becomes of concern (Rincón *et al.* 2020). This issue hinders adopting the piled raft foundation in soft soil condition. To increase the utilization of piled raft foundation system in soft ground, all above concerns need to be clarified and well understood.

This research presents the monitoring results and their interpretation of the pile foundation during the construction of a high-rise (124 m in height) building, "Navamindrapobitr 84th Anniversary Building" at Siriraj Hospital, Bangkok, in soft clayey ground. Axial forces in several piles, pore water pressure and earth pressures underneath the raft in a tributary area were monitored through the construction period of the building. The measurement data during the construction are interpreted and discussed. Three-dimensional (3D) finite element (FE) analyses are also performed to get more insight into the load sharing mechanism, and to evaluate the potential of utilizing the piled raft system in clayey ground.

2. Outline of building construction

2.1 Outline of building

The "Navamindrapobitr 84th Anniversary" Building (see Fig. 1(a)) has been being constructed from 2016 to 2019. The building has 24 stories and two basement floors with a building area of 3079 m^2, a total floor area of 75683 m^2, a height of 124.25 m and a basement level of -15.65 m below the ground surface (see Fig. 1(b)). The traditional bottom-up method was adopted for construction of the basement.

2.2 Site conditions

The construction site was located very close to Chao Phraya River, Bangkok, Thailand. The subsoil profile in the construction site is shown in Fig. 1c. The average values of undrained shear strength s_u and SPT-N are represented by red dash line and black solid line, respectively. The top 2.5 m thick layer is a soil crust, which is underlain by an 11.0 m thick soft clay layer. A stiff clay layer is found at a depth of 13.0 to 25 m below the ground surface. Beneath the stiff clay is hard clay having a thickness of approximately 4 m. The first sand layer is found at depths from 30 to 37 m.

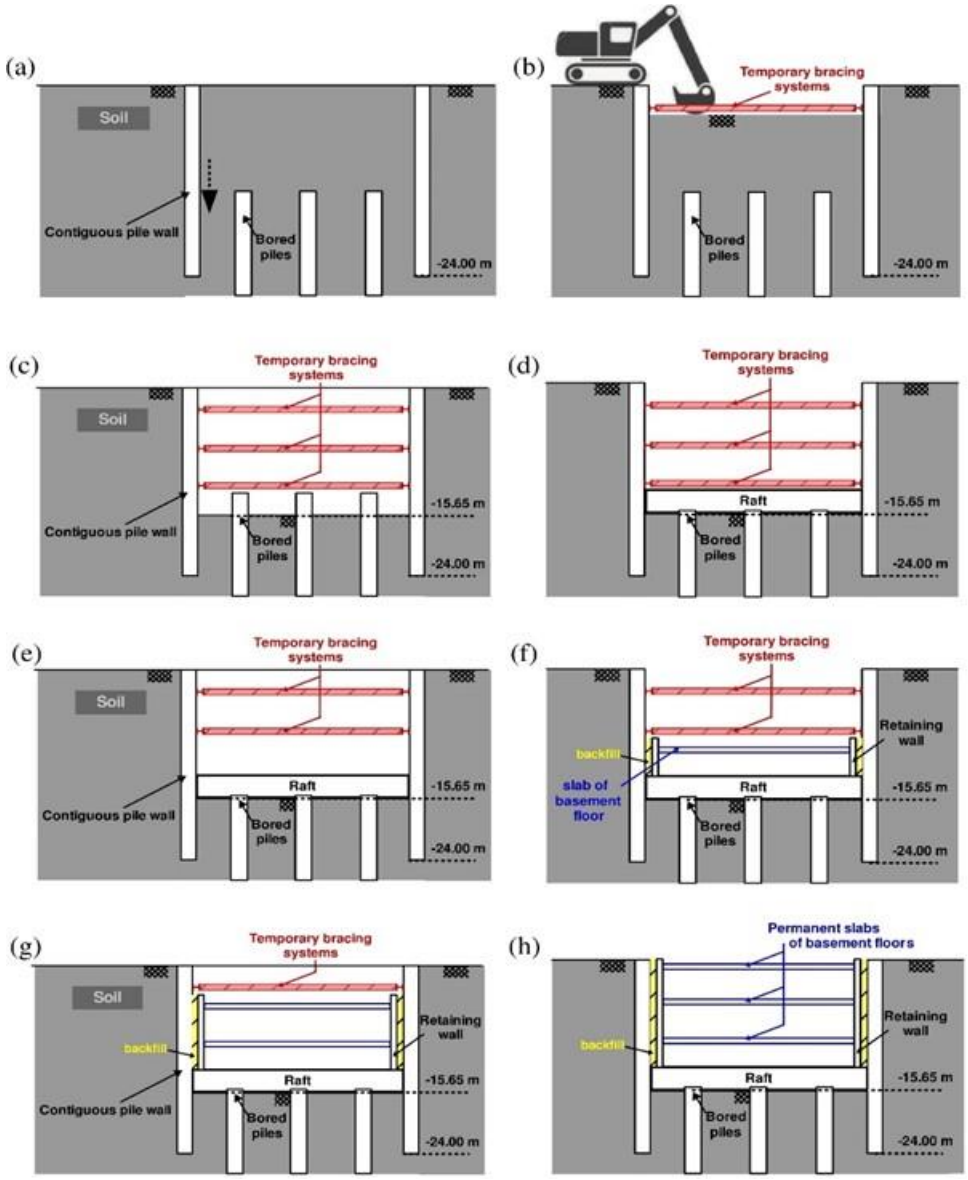

Fig. 2 Detail of underground construction sequences: (a) Construction of contiguous pile wall and bored piles, (b) Excavation and installation of bracing systems layer 1, (c) Excavation to -15.65 m, Installation of bracing systems layer 1, 2 and 3, (d) Construction of the raft foundation, (e) Removing bottom layer of strut L, (f) Construction of the basement B2, (g) Removing middle layer of strut L2 and (h) Completed underground structure

Below the upper first sand layer, there exist a hard clay and further down the 2nd dense sand layer. The ground water table is at 1.5 m below the ground surface. Due to the groundwater pumping in the past, the piezo-metric drawdown near the top level of the Bangkok stiff clay is found (MRTA 2017, Lueprasert *et al*. 2017). During the raft construction which was taken place in the stiff clay layer, no problem of ground water intrusion into the excavation pit has been found.

2.3 Construction sequence

A total of 350 cast-in-place concrete piles were constructed using a casing construction method. The bottom-up construction method was adopted for excavation and construction of basement floors and foundation of this building. Fig. 2 illustrates the bottom-up construction method employed in the construction of the foundation and the building. The sequence of pile foundation construction consists of 8 steps as follows:

• (a) Cast-in situ of reinforced concrete piles. Contiguous pile wall and bored piles were constructed at depths of 24 m and 25 m below the ground surface, respectively.

• (b) The soil is excavated to the first steel strut level in this case so-called “Strut Layer 1” (SL1) at 2.2 m.

• (c) The ground was excavated to a depth of 15.65 m (formation level) to expose the top of the pile foundation, and install steel Strut Level 2 (SL2) and Strut Level 3 (SL3) at depths of 6.5 m and 11.5 m, respectively.

• (d) Construction of the raft on the piles by cast-in situ of concrete in excavation area. In this case the raft contacts

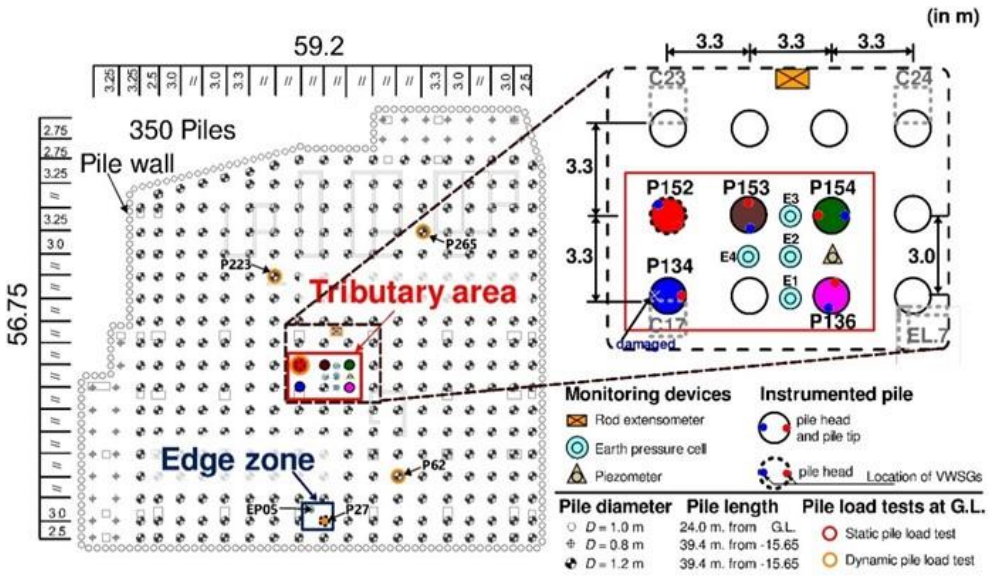

Fig. 3 Layout of piles, pile wall and location of monitoring devices

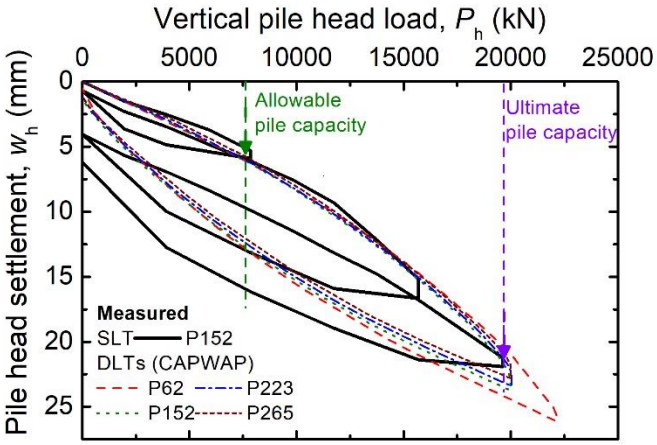

Fig. 4 The measured pile head load-displacement relation

directly to the piles, soil and contiguous pile wall.

• (e) Removing the bottom layer of strut (SL3). Note that the sides of raft contact directly to the pile wall. After the removal of strut, the force in strut can be transferred to the side of the raft.

• (f) Construction of the permanent slab of basement floor and retaining wall.

• (g) After removing the middle layer of strut (SL2), permanent basement slab and retaining wall are constructed.

• (h) Complete underground structure. Important dates for construction stages, starting after casting the raft were shown in Fig. 1(b).”

2.4 Design and construction of foundation

The layout of the piles is shown in Fig. 3. Among the total of 350 cast-in-place concrete piles, 318 piles had a diameter, D, of 1.2 m while 32 piles had a diameter of 0.8 m. The length of all the piles was 39.4 m, and the pile tips were embedded in the dense sand layer having SPT N-values of around 60 (Fig. 1(c)). The pile tips were thus at the elevation of -54.0 m from the ground surface. The pile wall had a diameter, D, of 1 m and the pile tips was embedded in stiff clay at the elevation of -24 m below ground surface. A 3.3m thick raft of reinforced concrete was placed on the stiff clay layer (SPT N-value of 20) at the depth of 15.65 m from the ground surface, after the completion of excavation work.

Static load test (SLT) was performed on a pile with D = 1.2 m (designated as P152) to confirm the designed load P_a of 7.85 MN. The measured load-displacement relation is shown in Fig. 4. At the maximum applied load of 19.6 MN (2.5 times of P_a), the corresponding pile displacement was 22 mm. According to the criterion of allowable maximum pile settlement of 25 mm as specified by the Department of Public works and Town & Country planning of Thailand (DPT) standard 1251 (DPT 2008), the P_a was confirmed from the test. Note that this design load is rather conservative.

Dynamic load tests (DLTs) were also conducted on 4 piles including P152. The load-displacement curves obtained from the wave matching analysis using CAPWAP (Pile Dynamics Inc. 2000) is indicated in Fig. 4. The curves of the 4 piles are similar to that obtained from SLT, showing

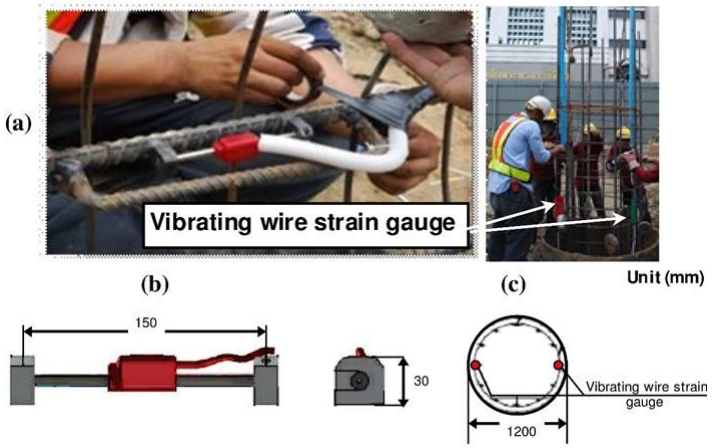

Fig. 5 The measured pile head load-displacement relation

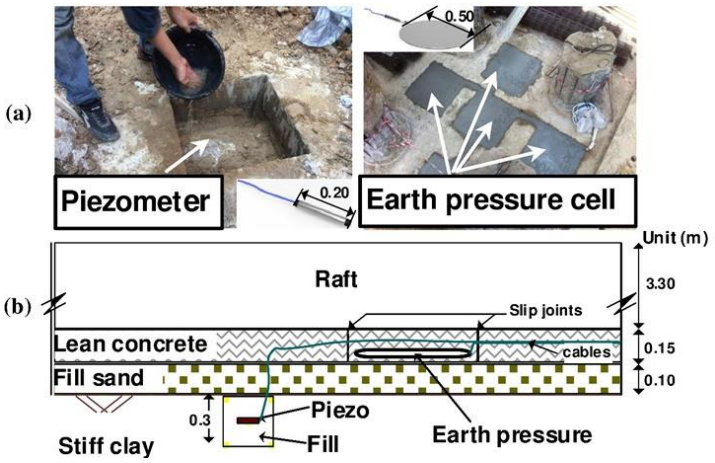

Fig. 6 Details on installation of piezometer and earth pressure cells: (a) photograph of piezometer and earth pressure cell in tributary area and (b) the layout of position of the instrumentations

that the performance of the piles is almost uniform in this building area.

SLT was not conducted on piles with D = 0.8 m. Hence, it was assumed that P_a of piles with D = 0.8 m is 44% of P_a of the pile with D = 1.2 m. That is, P_a of piles with D = 0.8 m is 3.5 MN. Note that the value of 44% corresponds to the ratio of cross-sectional area of the smaller diameter pile to that of the larger diameter pile.

The pile foundation was designed using the pile group concept, hence the maximum allowable load was estimated as 2608 MN. This is equivalent to the average allowable pressure of 847 kPa (including the self-weight of the raft) on the raft. Note that this designed load includes dead load from structure, load from heavy machines and equipment and designed live load. At the current stage, only the dead load of 400 kPa from structure was applied.

3. Instrumentations

In order to investigate the load sharing of the piles and the raft, axial forces in 5 piles, and earth pressures at 4 locations and pore water pressure at one location beneath the raft were monitored in the tributary area as shown in Fig. 3. Furthermore, axial force of a pile and earth pressure were monitored in the edge zone.

3.1 Monitoring of axial force of pile

Vibrating wire strain gauges (VWSGs) were instrumented in the monitored piles. A pair of VWSGs were attached on opposite sides of the reinforced bars (see Fig. 5) at both the pile head (-16.50 m) and pile tip (-54.00 m) levels for piles No. 134, 136, 153 and 154 in the tributary area. Pile No. 152 in the tributary area and pile No. 27 in the edge zone were instrumented with strain gauges only at the pile head level.

The axial force at each measurement level in pile was derived from Eq. (1), assuming that the deformation of the concrete and steel bars are compatible and no significant bending moment occurs in the plane orthogonal to the one containing the couple of strain gauges.

$$P = \varepsilon(E_c \times A_c + E_s \times A_s) \quad (1)$$

where ε is the average of measured axial strains, E_c and E_s are the Young's modulus of concrete and steel, A_c and A_s are the cross-sectional area of concrete and steel, respectively. Other alternative is to install the load cells as detailed in Russo and de Sanctis (2008).

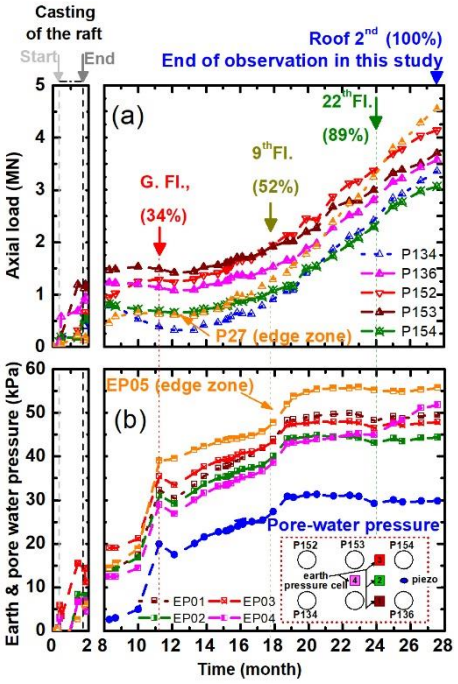

Fig. 7 Relationship between (a) Pile axial loads and (b) Earth & pore-water pressures versus time

3.2 Monitoring of pore water pressure and earth pressures underneath the raft

Vibrating wire piezometer having a diameter of 25 mm and earth pressure cells having a diameter of 500 mm were used to measure pore water pressure and earth pressures, respectively, as shown in Fig. 6.

During the installation of piezometer, water was poured into the excavated pit in which the piezometer was covered with sand fill to make the soil surrounding the piezometer fully saturated.

After the installation of the piezometers, the building area was covered by the sand layer having a thickness of 100 mm. Thereafter, a layer of lean concrete of 150 mm in thickness was constructed on the sand layer. The location of the earth pressure cell was isolated from the lean concrete layer using slip joints, so that pressure from the raft base is directly transferred to the earth pressure cell.

3.3 Method for estimating load sharing by piles and raft

In order to express the load sharing by the piles and the raft in the tributary area, the following quantities are used in this article:

$$q_{pile} = \frac{\sum F_{pile}}{A_T} \tag{2}$$

$$q_{raft} = \frac{\overline{p_{raft}} \times A_R}{A_T} \tag{3}$$

$$q'_{raft} = \frac{\overline{p_{raft}} \times A_R}{A_T} - p_w \tag{4}$$

$$q_{total} = \frac{\sum F_{pile}}{A_T} + \frac{\overline{p_{raft}} \times A_R}{A_T} = q_{pile} + q_{raft} \tag{5}$$

where $\sum F_{\text{pile}}$ = the sum of load carried by piles, $\overline{p_{\text{raft}}}$ = average raft pressure from 4 earth pressure cells, p_w = measured pore water pressure, q'_{raft}: effective raft pressure, A_T = area of tributary = 60 m^2 (6×10 m), A_R = area of raft = 53.21 m^2 (= A_T – A_P (area of piles = 6.79 m^2)), q_{total} = the sum of the pressures by piles and raft.

4. Results of field monitoring

4.1 Pile and raft loads

The development with elapsed time of the axial loads measured on the pile heads for six piles (five piles in the tributary area and one pile in the edge zone - see Fig. 3) are presented in Fig. 7(a). Fig. 7(b) presents the development with time of the earth and pore water pressures measured beneath the raft.

The construction of the raft was completed at 1.83 months. After that, removal of the main bracing system was done for 6 months, as mentioned in Section 2.3. During this period, monitoring data were smeared by this work for removing the bracing system.

It can be clearly seen that both the loads on the piles and the pressures generally increase with time as the construction continues. The measured pore water pressure beneath the raft was zero until 4.5 months. It is also seen that the changes of earth pressures are in accordance to that of the pore water pressure. This observation agrees well with the previous studies (Yamashita *et al.* 1991 and 2016).

From 0 to 1.83 months which is the construction period

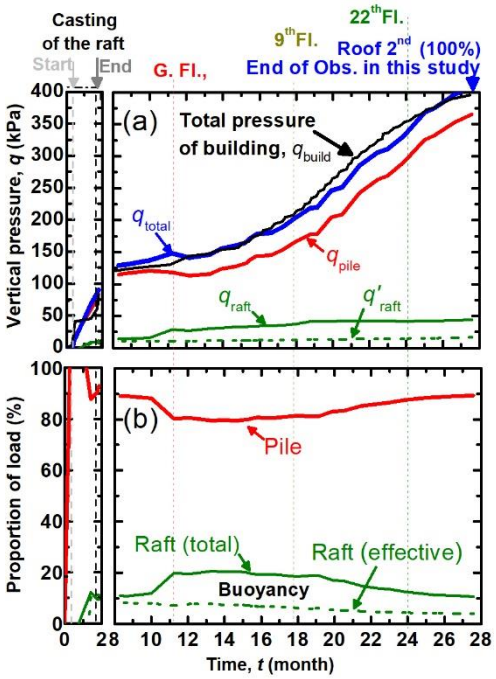

Fig. 8 Evolutions of (a) Vertical pressures and (b) Proportions of loads shared by the piles and the raft in the tributary area against time

of the raft, the increases of the pile load in the tributary area are significantly larger than the load on P27 in the edge zone. This is also true for the developments of the earth pressures in the tributary area and the edge zone.

After 8.3 months, the developments with time of the pile loads, pore water pressures and earth pressures can be categorized into four periods, including Period 1 from 8.3 to 11.3 months, Period 2 from 11.3 to 17.8 months, Period 3 from 17.8 to 24 months and Period 4 from 24 months to the end of measurement reported in this article which is 27.4 months. The construction sequence and the corresponding percentage of the final load in each period have been indicated in Fig. 1. In Period 1 (8.3 to 11.3 months), especially after 10 months, the rapid increases of the earth pressures as well as the ground water pressure are noticeably seen while the measured loads on the piles insignificantly increase or even decrease in some piles. This may be attributed to the gradual return of ground water table due to the low permeability of the stiff clay in which the raft is embedded. It is noticed that increment of the pore water pressure is almost equal to those of the earth pressures, indicating that most of increment of the applied load from the construction of superstructure is supported by the pore water pressure (the buoyancy force). The load on the piles was influenced by changes in the groundwater regime. This observation agrees with the monitoring results of Messeturm building, Frankfurt (Reul and Randolph 2004a). Note that the contribution from the swelling of soil may be expected (Poulos 1993). The upwards forces generated by the swelling of the clay due to the unloading has been reported by de Sanctis and Russo (2008) and Mandolini *et al*. (2005). However, with 5 months of excavation and preparation for foundation works in this project, the effect from the swelling of clay in this case is minimal.

In Period 2 (from 11.3 to 17.8 months) where the lower part of superstructure has been being constructed with a total load up to 52% of the final load, the pile loads, the earth pressures and the pore water pressure simultaneously increase. All the earth pressures in the tributary area increase with the same rate while a little bit smaller increasing rate of the earth pressure was measured at the edge zone. Note also that the earth pressure at the edge zone became the largest in Period 2, although it was smallest at the end of construction of the raft.

In Period 3 (from 17.8 to 24 months) in which the largest increment of the total load was applied, the behaviours of the pile loads, the earth pressures and the pore water pressure were different from those in the two previous periods. The pile loads increased continuously, while the earth pressures and the pore water pressure rapidly increased in a short period at the beginning before levelling off (keeping almost constant). It is also noticed that the magnitude of increases in earth pressures was generally the same with that of increase of the ground water pressure. After levelling off of the earth pressures, the increment of the construction load was entirely transferred to the piles.

In Period 4 (from 24 months to the last measurement reported herein), the tendency of the measured behaviours was similar to that in the previous period. The difference is a small decrease of the ground water pressure. It should be noted that the load transferred to the pile tip was almost zero at $t = 27$ months.

4.2. Load proportions between piles and raft

Fig. 8 shows the evolutions against time of (a) vertical

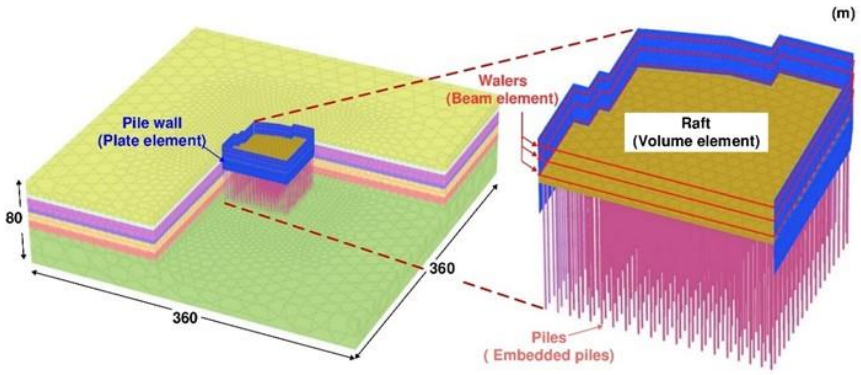

Fig. 9 Geometry of the problem and 3D finite element mesh used in this study

pressures and (b) proportions of loads shared by the piles and the raft in the tributary area. The quantities of q_{pile}, q_{raft}, q'_{raft} and q_{total} have been defined by Eqs. (2)-(5). The load from the superstructure divided by the foundation area is denoted by q_{build}.

The q_{total} is almost equal to the q_{build}, implying that the tributary area can adequately represent the behaviour of load transfer from the building to the foundation.

The followings can be found from Fig. 8(b):

• The proportion of the load by the piles (q_{pile}/q_{total}) was 90% at the end of construction of the raft.

• q_{pile}/q_{total} decreased with increasing buoyancy force and decreased to 80 % at the end of Period 1.

• q_{pile}/q_{total} remained almost unchanged until the end of Period 2.

• q_{pile}/q_{total} increased again in Periods 3 and 4 as the buoyancy force decreased and reached 90% at t = 27 months.

• The proportion of the load by effective pressure acting on the raft base (q'_{raft}/q_{total}) continued to decrease from the time of the end of raft construction to t = 27 months.

The proportion of the load carried by the piles (q_{pile}/q_{total}) was very high—around 80 to 90%. This is because the foundation was designed using the conventional approach where the contribution of the raft is not taken into account. The similar conclusion has also been reported by Russo (2018). Even for this design approach, 10 to 20% of the total load was supported by the raft in reality. A similar trend is also observed from field tests of building in stiff ground by Phung (2010) and Mandolini *et al*. (2005). This indicates that, by placing the raft to a greater depth at which the soil layer is sufficiently strong, the raft can be effective even in clayey ground condition.

5. Numerical analyses

As mentioned in Section 4, field measurements were carried out for only the tributary area and measurement of the settlements of the raft was not successful. In order to complement and extend the field monitoring results, three-dimensional (3D) Finite Element (FE) simulation of the whole foundation was conducted. Thereafter a series of parametric study was carried out to show the possibility of reducing number of piles with the concept of piled raft design.

5.1 Model mesh and boundary condition

In this study, 3D FE simulation of the pile foundation under increasing applied vertical pressure was conducted using the PLAXIS 3D version 2016 software. Fig. 9 depicts the FE modelling of the foundation system and the ground of the case study. The ground having a length of 360 m, a width of 360 m and a height of 80 m was modelled. Vertical and horizontal displacements at the bottom boundary of the ground were fixed. Horizontal displacements at the side boundaries of the ground were fixed.

The soil and the raft were represented by using ten-node tetrahedral volume elements. The bored concrete piles were modelled as embedded piles. The pile walls were modelled as plate elements. For the bracing system, the walers and struts were modelled as plate elements and beam elements, respectively. The construction load of superstructures was modelled as uniformly distributed loads on the top surface of the raft.

5.2. Back-analyses of pile load test and model parameters

In order to determine the soil parameters, back-analyses of the SLT of the tested pile was carried out prior to the analyses of the whole foundation. A SLT carried out on P152 as mentioned in Section 2.4 was simulated. The pile was modelled as a linear elastic material with the properties listed in Table 1. In this study, the pile was modelled as an embedded pile. The pile skin resistance was estimated using two widely used methods for pile design (α – method used to calculate the capacity of piles in layer of cohesive soils, β – method used to calculate the capacity of piles in layer of sand). Along the pile, surrounding soil by an interface with reduction factor R_{inter} of 1.0 is also modelled.

Based on the soil profile information, the materials for the 7 layers are summarized in Fig.10. The ground was modelled as Mohr-Coulomb type elastoplastic materials, which has been proven to be sufficient in previous study (e.g., Khanmohammadi and Fakharian 2018, Lueprasert *et al*. 2015). The soil parameters were estimated first based on the geotechnical investigation, and subsequently modified through the numerical analyses. Fully drained condition was assumed for the sand layers, while undrained condition was assumed for the clay layers. The soil properties, such as

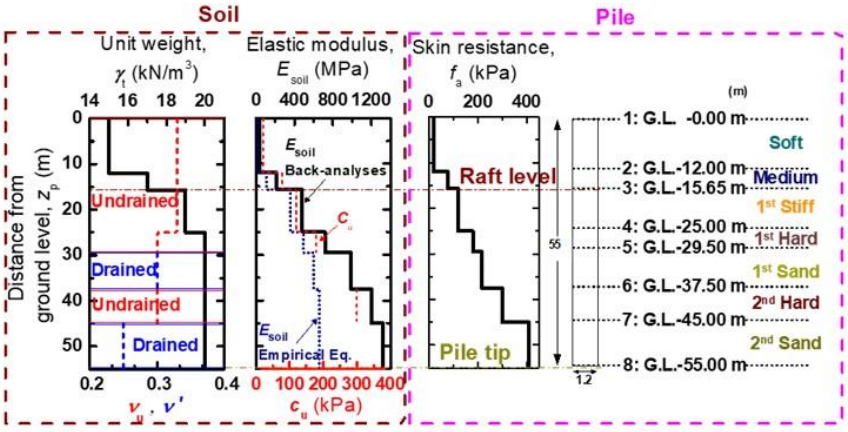

Fig. 10 Parameters of soil and pile-soil interface

Table 1 Structure model and parameter

Material	Type	Model	Length (m)	Cross sectional area (m^2)	Diameter/ Thick. (m)	Unit weight, γ (kN/m^3)	Young's modulus (kPa)	Poisson's ratio, ν
Bored pile	EBP	LE	39.5		1.2	8.0	2.65×10^7	
Raft	VE	LE			3.3	24.0	3.31×10^7	0.2
Pile wall	PE	LE	24		1	8.0	1.80×10^7	
Waler	BE	LE		0.04		75.0	2.00×10^8	

EBP: Embedded pile; VE: Volume element; PE: Plate element; BE: Beam element;
LE: Linear elastic

Table 2 Numerical simulation of the whole foundation

Stage	Construction activity	Construction time (months)	Applied pressure σ_v' (kPa)
1	In situ stress state	-	
2	Contiguous pile wall and pile foundation installations.	-	
3	Excavation to a depth of -2.9 m below ground level	-	
4	Install a temporary bracing system layer 1 (at -2.20m)	-	
5	Excavation to a depth of -7.2 m below ground level	-	
6	Install a temporary bracing system layer 2 (at -6.5m)	-	
7	Excavation to a depth of -12.5 m below ground level	-	
8	Install a temporary bracing system layer 3 (at -11.5m)	-	
9	Excavation to a depth of -15.65 m below ground level	-	
10	Install the raft at -15.65 m (thickness 3.3m) (self-weight)	0.00 – 1.83	-
11	Loading on raft (G. floor)	1.83 – 8.50	43
12^u	Loading on raft (1st floor)	8.50 – 11.26	52
13^u	Loading on raft (3rd floor)	11.26 – 14.86	79
14^u	Loading on raft (11th floor)	14.86 – 18.40	149
15^u	Loading on raft (16th floor)	18.40 – 20.90	206
16^u	Loading on raft (19th floor)	20.90 – 22.39	249
17^u	Loading on raft (22th floor)	22.39 – 23.90	273
18^u	Loading on raft (roof (E.O.C))	23.90 – 27.60	320

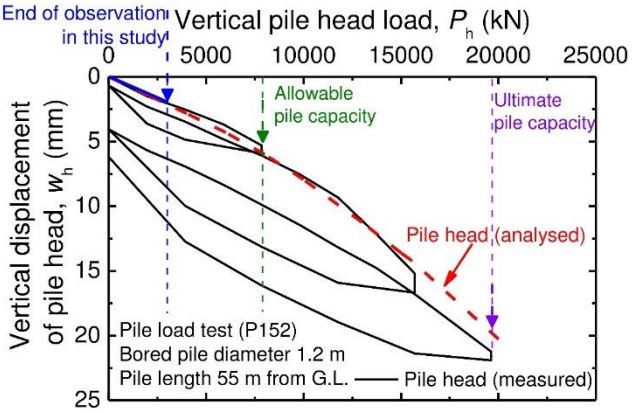

Fig. 11 Comparison of measured and analysed load-displacement curves of the test pile

Young's modulus and Poisson's ratio, were first estimated using empirical equations recommended by Imai and Tonouchi (1982) and Poulos *et al.* (2001). Note that the in-situ soil stiffness can be affected by the pile load test layout as revealed by Russo *et al.* (2013). For soft and medium soils, the undrained modulus, E_u, was approximately estimated to be 1050 to 1200 times of the undrained shear strength, s_u (Phienwej and Gan 2003), while an empirical equation $E_u = 1200 s_u$ was adopted for stiff and hard clays. For strength parameters in the Mohr-Coulomb model, cohesions c were determined from unconfined compression tests in soft clay and SPT values in stiffer clay where c of sands are assumed to be 1 kPa. The internal friction angle ϕ is equal to zero and 40° for the clay and for sand layers, respectively. The other parameters of the soil layers such as Poisson's ratio v are shown in Fig. 10.

Fig. 11 shows the comparison of the analysed and measured load-displacement curves of the tested pile. Good matching between the calculated and measured results was achieved when the Young's moduli of soils from empirical equation were adjusted as shown in Fig. 10.

5.3 The analysis procedure

Stage^U: considering the return of ground water

Table 2 outlines the step-by-step simulation of the construction process of the building in the finite-element

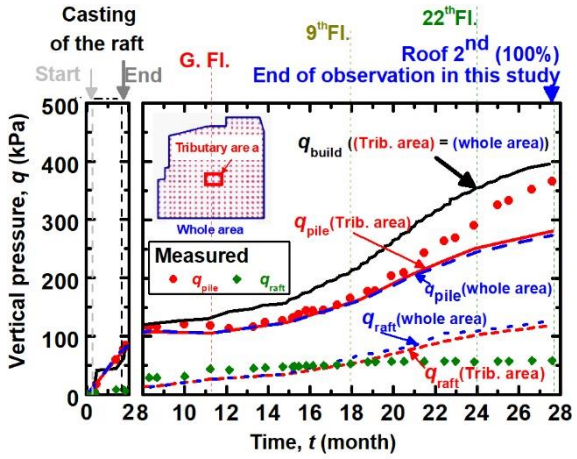

Fig. 12 Comparisons of measured (field case) and computed (tributary area and whole area) vertical pressures

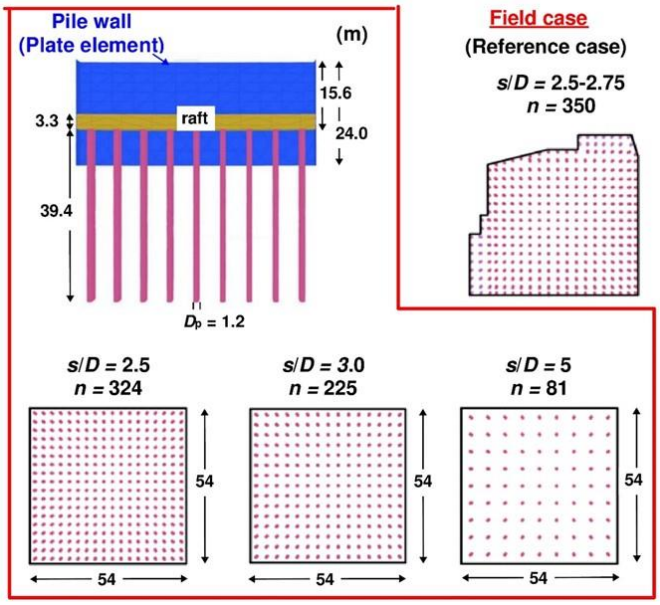

Fig. 13 System configurations in the numerical study

analysis. Firstly in stage 1, the self-weight analysis was performed to obtain the initial stresses of the ground. Stage 2 corresponds to the installation of contiguous pile walls and pile foundation before the excavation process. Stages 3 through 9 correspond to the excavation sequence and installation of the bracing system. The installation of the raft at -15.65 m (thickness 3.3 m) is performed in stage 10. The building construction pressure, σ'_v, was applied on the raft from 0-320 kPa in stages 11 to 18. As mentioned in Section 4, in Period 1 (8.3 to 11.3 months) especially after 10 months, the ground water table returns to the soil layer in which the raft is embedded. The pore pressure distribution following the observed piezometric pressure condition (see Fig. 1(c)) was considered in the analysis in stages 12 through 18.

5.4 FEM analyses of the whole foundation

Fig. 12 shows the comparisons between the measured and the computed vertical pressures shared by the piles (q_{pile}) and the raft (q_{raft}). The total vertical pressure q_{build} applied to the top surface of the raft is also included in the figure. Both the values considered in only the tributary area ($q_{(Trib.\ area)}$) and the whole area ($q_{(whole\ area)}$) are presented. The computed q_{pile} and q_{raft} are generally in good agreement with the measured ones indicating that the analysis procedure and parameters used are valid for further investigation of the pile foundation response under the construction load. Note that the q_{pile} is generally underestimated, particularly after 24 months. This is attributed to the consolidation process which has not been taken into account in this analysis. Previous numerical study on long term behaviour of piled raft (Yamashita *et al.* 2011, Watcharasawe *et al.* 2017, Hoang and Matsumoto 2020) reveal that the load shared by piles would increase in consolidation process.

In addition, both q_{pile} and q_{raft} calculated from the tributary area and those calculated from the whole area are also in good agreement showing that the load distribution in this building area is uniform. It also confirms again that

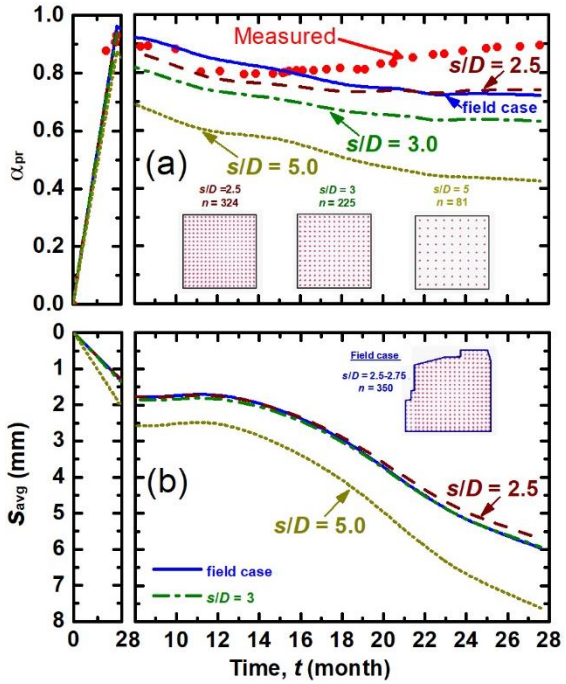

Fig. 14 Comparisons of measured (field case) and computed (field and reference cases) (a) load sharing ratio by piles and (b) average settlement versus time

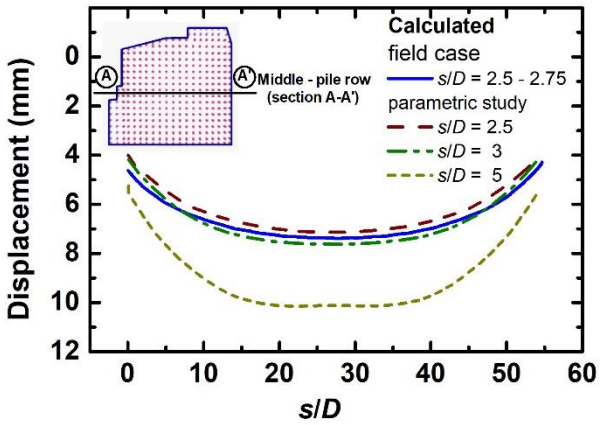

Fig. 15 Raft deflection along middle pile row of foundation

tributary area can adequately represent the behaviour of load transfer from the building to the foundation.

5.5 Parametric study

In order to evaluate the potential of implementing the piled raft as the foundation system for high-rise building in soft clayey ground, a series of parametric study analyses varying the number of piles are carried out. The load sharing and settlement behaviour of different piled raft configurations are investigated through the parametric study.

To reduce the complexity in the parametric study, a simple square building area was considered. Fig. 13 shows the system configurations considered in the parametric study. In addition to the prototype (reference field case), three different configurations having different numbers of piles (resulting to different pile spacing, *s/D*) were considered. All three cases possess the same building area of 54 × 54 m^2, the raft thickness of 3.3 m and the pile dimension (D_p = 1.2 m, L_p = 39.35 m). The piles were arranged to make *s/D* of 2.5, 3 and 5, respectively. The total number of piles can be seen in the figure. Note that the case with *s/D* of 2.5 is specified to have the equivalent *s/D* to the prototype (*s/D* = 2.50 to 2.75).

In this section, the main attention is paid to the bearing behaviour of the piled raft which is commonly described by the load sharing ratio by piles α_{pr}. The α_{pr} defines the ratio of the sum of load carried by piles to the total load of the building as follows:

$$\alpha_{pr} = \frac{\sum R_{pile,i}}{R_{tot}} \tag{6}$$

where α_{pr} = the load sharing ratio of piles; $\Sigma R_{pile,i}$ = the sum of all pile loads; R_{tot} = the total load of the structure (Mali

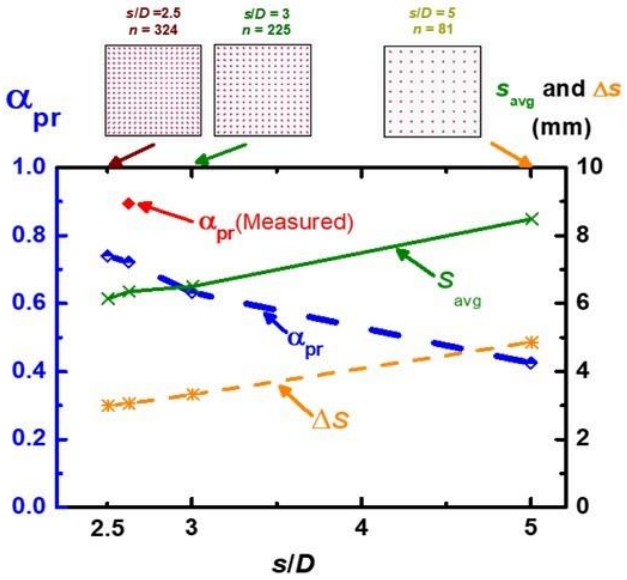

Fig. 16 Relationship between the load carried by pile, average settlement and differential settlement against the spacing of piles

and Singh 2018).

The computed α_{pr} from both the analyses and measurement are illustrated in Fig. 14(a). Fig. 14(b) depicts the evolution of computed settlement with time. The settlement increases with time as the construction load increases. The measured α_{pr} reveals that the weight of the raft during construction is gradually carried by the piles accompanying with settlement. After the raft was casted, construction load from the following steps is shared by both the raft and piles while settlement insignificantly increases during 8th-14th month (not much increasing load in this period). After this, the settlement gradually increases again as the construction load increases. It is seen that the computed α_{pr} of the prototype case has generally good agreement with the measurement in both the tendency and magnitude, although smaller predicted values can be noticed after 16 months. It is seen that the raft can share the load up to 20% during construction. At the end of construction, the measured results indicate that the load share by raft of 10% is seen, even though the foundation has been designed considering that all load will be carried by the piles. Note that the live load has not been fully applied yet at the end of construction stage.

In the parametric study, with decreasing number of piles from 324 to 81, α_{pr} decreases from 0.73 to 0.42. It indicates that the load shared by raft can be increased up to 58%. However, larger settlement must be sacrificed. It is also noticed that the rate of decrease of α_{pr} with construction progress increases with s/D, especially from 17.8 to 24 months in which the largest increment of the total load was applied.

Fig. 15 shows the computed settlements of the raft in the section of middle pile-row (A-A') of the foundation at the end of construction. For all the cases, the settlements are largest at the centre of the raft and gradually become smaller to the edge. For the prototype case, the settlement in the range of 5 to 8 mm can be seen. Considering the allowable maximum settlement which is usually 25 mm, this range of settlement is very low. This implies that larger settlement of the building can be allowed. This can be done by reducing the number of piles. By reducing the number of piles to s/D of 5.0, the settlements of the foundation drastically increase. This reveals that the large settlements are necessarily sacrificed if smaller number of piles is preferred to enhance the raft performance which agrees well with previous study (de Sanctis *et al.* 2002, Fioravante *et al.* 2008, Amornfa *et al.* 2012, Reul 2004, Mali and Singh 2018). However, the computed maximum settlement for case with s/D of 5.0 is still lower than the allowable value.

The computed α_{pr} at the end of construction of all configurations considered in this study are plotted in Fig. 16. The average and differential settlements of the foundation are also shown in the figure.

The average foundation settlement s_{avg} and differential settlement Δs from the 3D-FE analyses were calculated by the following equations by Reul and Randolph (2004b):

$$s_{avg} = (2s_{center} + s_{corner}) / 3 \quad (7)$$

$$\Delta s = s_{center} - s_{corner} \quad (8)$$

where s_{center} and s_{corner} are the raft settlements at centre and corner, respectively.

For the case with s/D of 5.0, the α_{pr} decreases to 0.5, meaning that the raft shares a half of the total load. This high level of load sharing by raft is also reported in previous numerical analysis of piled raft in stiff ground (Reul 2004, Mali and Singh 2018). The s_{avg} and Δs increases with increasing s/D. It is noticed that the rates of increasing s_{avg} and Δs against s/D are approximately the same.

6. Conclusions

Comprehensive field monitoring of the pile foundation during the construction of a high-rise (124 m in height) building was carried out and the results were interpreted and discussed in this paper. Three-dimensional (3D) finite element (FE) analyses were also performed to get more insight into the load sharing mechanism, and to evaluate the potential of using the piled raft system in soft clayey ground. The main conclusions are as follows:

• Even though the foundation has been designed using conventional approach of pile group with a high factor of safety, the raft of the pile foundation in clayey ground can share the load up to 10%.

• The merits of pile foundation in soft clayey ground whose permeability is low, can be realized. The return of ground water at a certain time after construction results to the increase of load shared by raft by means of uplift pressure.

• For the prototype case, the computed settlement in the range of 5 to 8 mm can be seen. Considering the allowable maximum settlement which is usually 25 mm, this range of settlement is very low. This implies that larger settlement of

the building can be allowed. This can be done by reducing the number of piles.

• In numerical analyses, if the number of piles is reduced from 324 to 81, α_{pr} decreased from 0.73 to 0.42. It indicates that the raft can share a half of the total load.

• The potential of utilizing the piled raft system for high-rise building with underground basement in soft clayey ground is thus preliminarily confirmed.

This study considers only the short term behaviour. At the current stage, only the dead load from the structure with the safety factors of 6.6 with respect to the ULS of the design, was applied to the piles. The future work considering the service load and the long-term condition with regard to the consolidation and ground water return should be done to confirm the potential of using this system in soft clayey ground condition. The long-term monitoring has currently been being performed by the authors.

Acknowledgments

The authors gratefully acknowledge the financial support by Thailand Research Fund (TRF) and Geotechnical & Foundation Engineering Co., Ltd. (GFE) through the TRF-RRi Project under Contract No 58I0050 and National Research Council of Thailand through grant No. NRCT5-RSA63006. The authors also wish to thank the International Project Administration Company Limited for their supports in field instrumentations. The guidance and contribution of Associate Professor Kasem Petchgate, former Dean of Faculty of Engineering, KMUTT and President of Kasem Design and Consultant Co. Ltd., are gratefully acknowledged. Thanks are also extended to Siriraj Hospital, Plan Consultants Co., Ltd. and Westcon Co., Ltd.

References

Amornfa, K., Phienwej, N. and Kitpayuck, P. (2012), "Current practice on foundation design of high-rise buildings in Bangkok, Thailand", *Lowl. Technol. Int.*, **14**(2), 70-83. https://doi.org/10.1016/j.humov.2017.02.008.

de Sanctis, L. and Mandolini, A. (2006), "Bearing capacity of piled rafts on soft clay soils", *J. Geotech. Geoenviron. Eng.*, **132,** 1600-1610. https://doi.org/10.1061/(ASCE)1090-0241(2006)132:12(1600).

de Sanctis, L. and Russo, G. (2008), "Analysis and performance of piled rafts designed using innovative criteria", *J. Geotech. Geoenviron. Eng.*, **134**(8), 1118-1128. https://doi.org/10.1061/(ASCE)1090-0241(2008)134:8(1118).

de Sanctis, L., Mandolini, A., Russo, G. and Viggiani, C. (2002), "Some remarks on the optimum design of piled rafts", *Proceeding of the International Deep Foundations Congress 2002*, Orland, Florida, U.S.A., February.

DPT standard 1251. (2008), Standard for testing pile by static load, Department of public works and town country planning Thailand, Bangkok, Thailand.

Fattah, M.Y., Al-Mosawi, M.J. and Al-Zayadi, A.O. (2013), "Time dependent behavior of piled raft foundation in clayey soil", *Geomech. Eng.*, **5**(1), 17-36. https://doi.org/10.12989/gae.2013.5.1.017.

Fioravante, V., Giretti, D. and Jamiolkowski, M. (2008), "Physical modeling of raft on settlement reducing piles", *Prceedings of the Symposium Honoring Dr. John H. Schmertmann for His Contributions to Civil Engineering at Research to Practice in Geotechnical Engineering Congress 2008*, New Orleans, Louisiana, U.S.A., March.

Hoang, L.T. and Matsumoto, T. (2020), "Long-term behavior of piled raft foundation models supported by jacked-in piles on saturated clay", *Soils Found.*, **60**(1), 198-217. https://doi.org/10.1016/j.sandf.2020.02.005.

Imai, T. and Tonouchi, K. (1982), "Correlation of N-value with S-wave velocity and shear modulus", *Proceedings of the 2nd European Symposium of Penetration Testing*, Amsterdam, The Netherlands.

Kakurai, M., Yamashita, K. and Tomono, M. (1987), "Settlement behavior of piled raft foundation on soft ground", *Proceedings of the 8th Asian Regional Conference on Soil Mechanics and Foundation Engineering*, Kyoto, Japan.

Katzenbach, R., Arslan, U. and Moormann, C. (2015), "Piled raft foundation projects in Germany", *Des. Appl. Raft Found.*, 323-391. https://doi.org/10.1680/daorf.27657.0013.

Khanmohammadi, M. and Fakharian, K. (2018), "Evaluation of performance of piled-raft foundations on soft clay: A case study", *Geomech. Eng.*, **14**(1), 43-50. https://doi.org/10.12989/gae.2018.14.1.043.

Ko, J., Cho, J. and Jeong, S. (2018), "Analysis of load sharing characteristics for a piled raft foundation", *Geomech. Eng.*, **16**(4), 449-461. https://doi.org/10.12989/gae.2018.16.4.449.

Lueprasert, P., Jongpradist, P., Charoenpak, K., Chaipanna, P. and Suwansawat, S. (2015), "Three dimensional finite element analyses for preliminary establishment of tunnel influence zone due to nearby pile loading", *Maejo Int. J. Sci. Tech.*, **9**(2), 209-223. https://doi.org/10.14456/mijst.2015.16.

Lueprasert, P., Jongpradist, P., Jongpradist, P. and Suwansawat, S. (2017), "Numerical investigation of tunnel deformation due to adjacent loaded pile and pile-soil-tunnel interaction", *Tunn. Undergr. Sp. Tech.*, **70**, 166-181. http://doi.org/10.1016/j.tust.2017.08.006.

Mali, S. and Singh, B. (2018), "Behavior of large piled-raft foundation on clay soil", *Ocean Eng.*, **149**, 205-216. https://doi.org/10.1016/j.oceaneng.2017.12.029.

Mandolini, A., Russo, G. and Viggiani, C. (2005), "Pile foundations: Experimental investigations, analysis and design", *Proceedings of the 14th International Conference on Soil Mechanics and Geotechnical Engineering*, Osaka, Japan.

MRTA. (2017), "Soil Investigation Report: The MRT orange line (east section) Project contract E1: underground civil works", Mass Rapid Transit Authority of Thailand, Bangkok, Thailand.

Phienwej, N. and Gan, C.H. (2003), "Characteristics of ground movement in deep excavations with concrete diaphragm walls in Bangkok soils and their prediction", *Geotech. Eng.*, **34**, 167-175.

Phung, L.D. (2010), "Piled Raft – A cost-effective foundation method for high-rises", *Geotech. Eng.*, **41**, 1-12.

Pile Dynamics Inc. (2000), *CAPWAP for Windows Manual*, Cleveland, Ohio, U.S.A.

Poulos, H.G. (1993), "Piled rafts in swelling or consolidating soils", *J. Geotech. Eng.*, **119**(2), 374-380. https://doi.org/10.1061/(ASCE)0733-9410(1993)119:2(374).

Poulos, H.G. (2001), "Piled raft foundations: Design and applications", *Géotechnique*, **51**, 95-113. https://doi.org/10.1680/geot.51.2.95.40292.

Poulos, H.G., Carter, J.P. and Small, J.C. (2001), "Foundations and retaining structures-research and practice", *Proceedings of the 15th International Conference on Soil Mechanics and Geotechnical Engineering*, Istanbul, Turkey, August.

Randolph, M.F. (1994), "Design methods for pile groups and piled rafts", *Proceedings of the 13th International Conference on Soil*

Mechanics and Foundation Engineering, New Dehli, India, January.
Reul, O. (2004), "Numerical study of the bearing behavior of riled rafts", *Int. J. Geomech.*, **4**, 59-68. https://doi.org/10.1061/(ASCE)1532-3641(2004)4:2(59).
Reul, O. and Randolph, M.F. (2004a), "Piled rafts in overconsolidated clay: comparison of in situ measurements and numerical analyses", *Géotechnique*, **53**, 301-315. https://doi.org/10.1680/geot.2003.53.3.301.
Reul, O. and Randolph, M.F. (2004b), "Design strategies for piled rafts subjected to nonuniform vertical loading", *J. Geotech. Geoenviron. Eng.*, **130**, 1-13. https://doi.org/10.1061/(ASCE)1090-0241(2004)130:1(1).
Rincón, E.R., da Cunha, R.P. and Caicedo, B. (2020), "Analysis of settlements in piled raft systems founded in soft soil under consolidation process", *Can. Geotech. J.*, **57**(4), 537-548. https://doi.org/10.1139/cgj-2018-0702.
Russo, G. (1998), "Numerical analysis of piled rafts", *Int. J. Numer. Anal. Meth. Geomech.*, **22**(6), 477-493. https://doi.org/10.1002/(SICI)1096-9853(199806)22:6<477::AID-NAG931>3.0.CO;2-H.
Russo, G. (2012), "Experimental investigations and analysis on different pile load testing procedures", *Acta. Geotech.*, **8**(1), 17-31. https://doi.org/10.1007/s11440-012-0177-4.
Russo, G. (2018), "Analysis and design of pile foundations under vertical load: An overview.", *Rivista Ital. Geotecnica*, **52**(2), 52-71. https://doi.org/10.19199/2018.2.0557-1405.52.
Russo, G., Abagnara, V., Poulos, H.G. and Small, J.C. (2013), "Re-assessment of foundation settlements for the Burj Khalifa, Dubai", *Acta. Geotech.*, **8**(1), 3-15. https://doi.org/10.19199/2018.2.0557-1405.52.
Sales, M.M., Small, J.C. and Poulos, H.G. (2010), "Compensated piled rafts in clayey soils: Behaviour, measurements, and predictions", *Can. Geotech. J.*, **47**, 327-345. https://doi.org/10.1007/s11440-012-0193-4.
Tan, Y.C., Cheah, S.W. and Taha, M.R. (2006), "Methodology for design of piled raft for 5 story buildings on very soft clay", *Proceedings of the GeoShanghai International Conference 2006*, Shanghai, China, June.
Watcharasawe, K., Kitiyodom, P. and Jongpradist, P. (2015), "Numerical analyses of piled raft foundation in soft soil using 3D-FEM", *Geotech. Eng.*, **46**, 109-116. https://doi.org/10.1111/j.1746-1561.2007.00159.x.
Watcharasawe, K., Kitiyodom, P. and Jongpradist, P. (2017), "3-D Numerical analysis of consolidation effect on piled raft foundation in Bangkok subsoil condition", *Int. J. Geomate*, **12**, 105-111. https://doi.org/10.21660/2017.31.6529.
Yamashita, K. and Kakurai, M. (1991), "Settlement behavior of raft foundation with friction piles", *Proceeding of the 4th International Conference on Piling Deep Foundations*, Stresa, Italy, April.
Yamashita, K., Hamada, J. and Yamada, T. (2011), "Field measurements on piled rafts with grid-form deep mixing walls on soft ground", *Geotech. Eng.*, **42**, 1-10.
Yamashita, K., Hamada, J. and Tanikawa, T. (2016), "Static and seismic performance of a friction piled raft combined with grid-form deep mixing walls in soft ground", *Soils Found.*, **56**, 559-573. https://doi.org/10.1016/j.sandf.2016.04.02.